TECHNICAL TRANSACTIONS 12/2017
CZASOPISMO TECHNICZNE 12/2017
CHEMISTRY
DOI: 10.4467/2353737XCT.17.212.7755

Tomasz M. Majka (tomasz.majka@pk.edu.pl)
Agnieszka Leszczyńska
Krzysztof Pielichowski
Department of Chemistry and Technology of Polymers, Faculty of Chemical Engineering and Technology, Cracow University of Technology.

Mechanical properties vs biotic degradation of polyamide/layered silicates nanocomposites

Właściwości mechaniczne vs degradacja biotyczna nanokompozytów poliamid/krzemiany warstwowe

Abstract

The purpose of this study was to obtain polyamide 6 nanocomposites with different organically modified clays and to study the biotic degradation behaviour vs mechanical properties of the obtained materials. Thermal stability of pure organoclays was investigated using thermogravimetric analysis (TGA). The prepared nanocomposites were characterized by X-ray diffraction (XRD) and infrared spectroscopy (IR). The evolution of mechanical properties was also studied. The obtained results confirm good interactions of nanofillers with the polymer, showing the formation of intercalated and/or partially exfoliated structures. The nanocomposites showed higher thermal stability compared to pure polymer, and advantageous mechanical properties. Finally, a discussion related to the effects of biotic degradation on mechanical properties of PA6/MMT nanocomposites is presented.

Keywords: polymer nanocomposites, polyamide 6, layered silicates, montmorillonite, biotic degradation

Streszczenie

Celem przeprowadzonych badań było otrzymanie nanokompozytów poliamidowych z różnym typem organicznie modyfikowanej glinki. Stabilność termiczna czystych glinek mierzono za pomocą analizy termograwimetrycznej (TGA). Otrzymane nanokompozyty zostały scharakteryzowane przy wykorzystaniu dyfrakcji promieni rentgenowskich (XRD) oraz spektroskopii w podczerwieni (IR). Zbadano również zmiany własności mechanicznych. Uzyskane wyniki potwierdzają dobrą interkalację nanonapełniaczy z matrycą polimerową, pokazując tworzenie struktur częściowo eksfoliowanych. Nanokompozyty wykazały wyższą stabilność termiczną w porównaniu do czystego poliamidu. Artykuł zamyka dyskusja związana ze skutkami degradacji biotycznej nanokompozytów PA6/MMT na ich właściwości mechaniczne.

Słowa kluczowe: nanokompozyty polimerowe, krzemiany warstwowe, poliamid 6, montmorylonit

1. Introduction

The search for the new hybrid polymer materials with improved processability and better thermal properties than commercially available polymers has received significant attention from both academia and industry. In the last 20 years, natural clay–polymer nanocomposites have become an active field of research because of their unique microstructures and enhanced properties. However, in some areas of industry, there is a great demand for materials with improved functional properties relative to those on the market. The growing needs are related primarily to the military sector, automotive and packaging, where high demands are made for polymer products [1–7]. New applications involve a need to develop innovative solutions or modification of polymer materials produced. The growing interest is focused on polymeric nanocomposites, i.e. materials, consisting of two separable phases: a continuous phase (matrix) and a dispersed phase comprised of nanoparticles having at least one dimension less than 100 nm [1-3]. The improvement of certain properties allows functional or structural nanocomposites to be obtained. Among different nanofillers, special attention was paid to layered silicates, particularly montmorillonite (MMT). Extensive studies have shown that proper dispersion of particles of montmorillonite in a polymer matrix can result in improved mechanical, thermal, barrier and flame retardant properties [2–7]. Polyamide 6 nanocomposites with montmorillonite, although well-known, suffer from thermo-oxidative degradation and flammability [8–11].

It is well known that MMT can substantially improve thermoplastic polymer matrix properties even at a low load (3-5%) of the nanofiller [12]. Wu et al. [13] reported that modulus, bending strength and heat distortion temperature of these nanocomposites increased with increasing clay content, and tensile strength increased up to 4.3 wt% and then decreased with further increases of montmorillonite content in PA6/organoclay nanocomposites prepared by melt compounding. Another study [14] showed that both nanocomposites prepared with 1% and 3% of MMT were exfoliated, but at 5% load MMT was intercalated among two basal planes of MMT, leading to an expansion of the interlayer spacing. However, the thermogravimetric results indicated that the nanocomposites showed largely higher thermal stability compared to the pure polymer.

Current studies are focused on e.g. biopolymer/clay nanocomposites [15] or polyamide /polyolefin/clay blend nanocomposites [16]. Although numerous studies have been devoted to polyamide/MMT nanocomposites, the problems associated with biotic degradation behaviour vs mechanical properties changes have not been sufficiently addressed.

The aim of this work is to analyse the structure, morphology, thermal stability and mechanical properties of polyamide/montmorillonite (PA6/MMT) nanocomposites subjected to biotic degradation. The nanocomposites were prepared by the melt intercalation method, where three different clays were used. Each of the clays was characterized by thermogravimetric analysis (TGA) and only two of them were recommended for processing with PA6. The prepared nanocomposites were then characterized by X-ray diffraction (XRD) and infrared spectroscopy (IR). The mechanical properties – flexural strength – of PA6/MMT nanocomposites after long-term biotic degradation have been determined.

2. Experimental

2.1. Materials

The nanocomposites were produced using a PA6 melt-compounded with three types of organo-modified montmorillonites (OMMT), developed for extrusion compounding with PA6. Dellite® 43B (D43B), supplied by Laviosa, was a dimethyl-benzyl-hydrogenated tallow ammonium salt modified clay; Dellite® 72T (D72T) was a dimethyl-di(hydrogenated tallow) ammonium salt modified clay with low modifier content. Nanomer® I30P (NI30P), supplied by Nanocor, was a clay organofilized with high content of dimethyl-di(hydrogenated tallow) ammonium salt. The PA6 (Tarnamid® T30), supplied by Grupa Azoty SA, was a high-viscosity extrusion grade PA designed for technical applications.

2.2. Sample preparation

Before the preparation of nanocomposites, the materials were dried in a laboratory vacuum oven. Polyamide was dried at 80°C for 3 hours. Dried matrix and 3 wt% of nanofiller were mechanically premixed then compounded using a twin co-rotating screw extruder Thermo Scientific Rheomex PTW 16/25 XL with a screw speed of 150 rpm, a temperature profile in the range of 245°C (feed throat) to 260°C (die). The compounds were extruded as single fibre of 4 mm diameter, which was hauled into a quenching water trough prior to being pelletized (Table 1).

Table 1. Processing conditions of PA6/MMT nanocomposites

Twin co-rotating screw extruder								
Feeder performance (%)	Rotational speed (rpm)	Heating zones						
		1	2	3	4	5	6	Die
0.3	150							
Temperature (°C)		245	245	245	250	255	250	260
Atmospheric venting		-------	-------	-------	-------	YES	-------	-------
Length of the zones (mm)		80	60	60	64	60	76	23
L/D		5.00	3.75	3.75	4.00	3.75	4.75	-------
Cooling tank								
Length of cooling surface (mm)		1500						
Tank volume (dm^3)		27						
Height of bath (mm)		1081						
Water temperature (°C)		18						
Pelletizer								
Size of pellets (mm)		1						
Rotational speed (1/s)		12						

The dried nanocomposites were moulded to form flexural bar specimens using a Zamak WT12 injection moulding machine. The cylinder temperature profile was 232°C and the mould temperature was maintained at 90°C. To minimize moisture uptake moulded specimens were immediately wrapped in aluminium foil and sealed in polyethylene bags. Prior to mechanical testing, all specimens were dried for 3 h at 80°C and then conditioned in a dessicator for a minimum of 3 days.

2.3. X-Ray Diffraction (XDR)

X-ray diffraction (XRD) measurements were performed using an X-ray powder diffractometer Phaser D2 with a Cu Kα2 (λ=1.54 Å). Measurements were made in two systems:

- in the range of 5–40° angle 2θ – a gap of 1 mm and an aperture of 3 mm in the trading system with step 0.5 at 180°;
- in the range of 0.5–3° angle 2θ – a gap of 0.2 mm and an aperture of 1 mm in the stationary system.

2.4. Infrared spectroscopy (IR)

Studies using Fourier transform infrared spectroscopy (FTIR) were performed in reflectance mode using a Perkin Elmer Spectrum 65 spectrometer with ATR accessory (diamond crystal / ZnSe – spectral range 4000 - 650 cm^{-1}, penetration depth ~2 microns, number of scans 32 , resolution 4 cm^{-1});

2.5. Thermal analysis

Thermogravimetric measurements were made using a thermogravimetric analyser Netzsch TG 209. Measurements were carried out using the following measurement conditions:

- Measurement temperature range of 20°C-605°C;
- Heating rate of 10°C/min;
- Oxidizing environment, air flow of 15cm^3/min.

In each case, the measuring corundum (α-Al_2O_3) cell was open and the mass of the sample ~5 mg.

Thermal conversion of PA6/OMMT nanocomposites was investigated by Differential Scanning Calorimetry using a Mettler Toledo DSC823^e calorimeter. Calorimetric measurements were carried out in an oxidizing atmosphere. The calorimeter was calibrated using indium and zinc standards. The sample (ca. 10 mg) was placed in an aluminium pan, and sealed in the press. The measurements were performed according to the two programs that allowed the evaluation of thermal properties:

- Heating from -30 to 300°C at 20°/min;
- Cooling from 300 to -30°C at 5°/min.

2.6. Mechanical tests

The static flexural strength of the nanocomposites was recorded using a universal testing machine Zwick Z005 TH in accordance with DIN EN ISO 178, and with a deformation speed of 2 mm / min. Tests were carried out at three temperatures: 0, 25 and 80°C. The reported values of strength were the arithmetic average of at least eight measurements. As a result of the test, $\sigma = f(\varepsilon)$ curves and the bending modulus values, flexural bending stress, flexural strength, elongation area at the bending strength and the bending stress at failure were obtained.

2.7. Biotic degradation

Biotic degradation was carried out for 475 days. The PA6/OMMT composite panels were obtained by compression press (Zamak P-200) with heated punches. Press conditions were as follows: press temperature – 230°C; time of process – 5 minutes; compression pressure – 25 bar. Collected plates with dimensions 100x100x10 mm were screwed together by screws to form a cube. The composite cube was buried underground at a depth of 1 metre in the ground with pH of ca. 6.8.

3. Results and discussion

3.1. TGA of fillers

Fig. 1 shows thermogravimetric curves of commercial organoclays. For all tested clays, content of absorbed moisture oscillates around 2–3%. The course of TG curves reveals two decomposition stages. The first stage of degradation in the range up to approx. 200°C is related to the evaporation of water and the emission of low molecular weight modifier compound present in the system.

Depending on the type of quaternary salt, the onset and end temperatures of the first stage differ; to compare the results of thermogravimetric analysis, representative indices of 5, 10, 20%, and the maximum weight loss, have been identified – Table 2.

Table 2. Weight loss parameters of organoclays

Sample	$T_{5\%}$ [°C]	$T_{10\%}$ [°C]	$T_{20\%}$ [°C]	T_{max} [°C]	T_{onset} [°C]
Dellite® 43B	211	232	288	227	197
Dellite® 72T	253	283	337	298	245
Nanomer® I30P	306	340	502	340	292

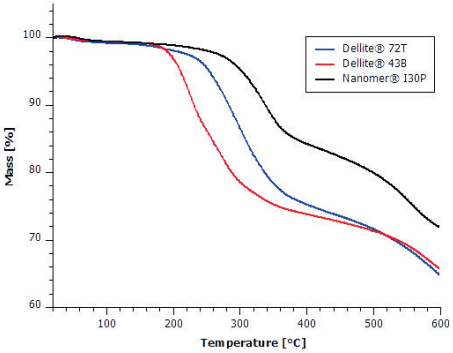

Fig. 1. Thermogravimetric curves of commercial organoclays

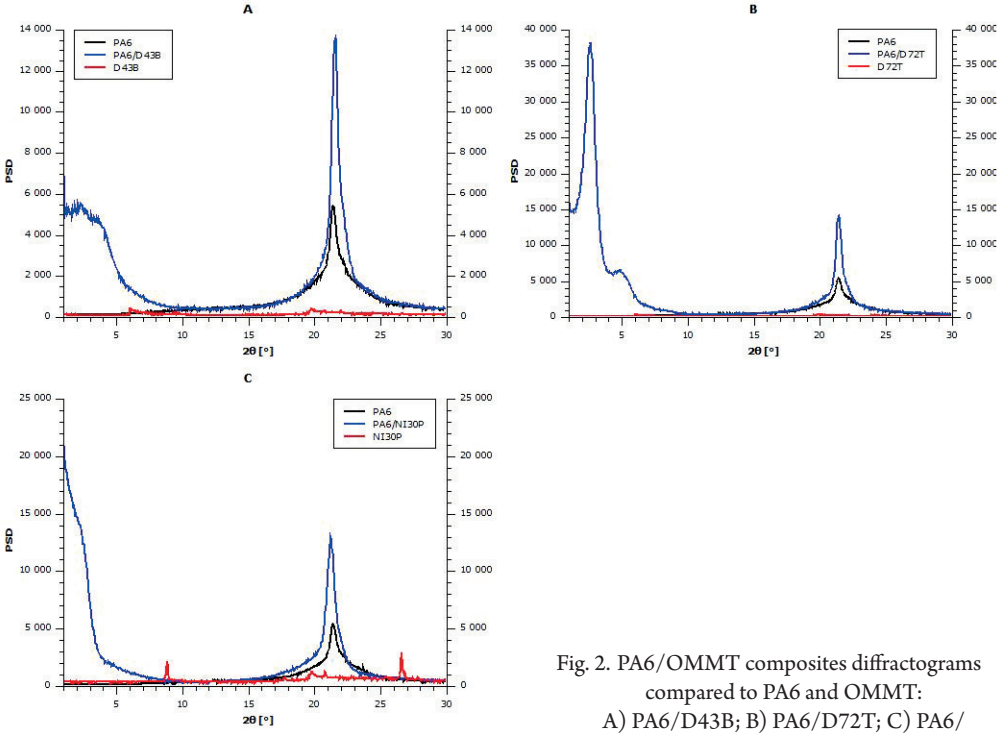

Fig. 2. PA6/OMMT composites diffractograms compared to PA6 and OMMT: A) PA6/D43B; B) PA6/D72T; C) PA6/NI30P

Among the clays, the lowest value of weight loss reached montmorillonite modified with dimethyl-benzyl-hydrogenated tallow ammonium salt. On the other hand, the highest values of the indicators were found for NI30P. The second stage of degradation in the range of 400-600°C may be linked to decomposition reactions resulting in the formation of low molecular weight compounds.

3.2. X-Ray Diffraction (XDR)

The analysis of the XDR results allowed information to be acquired on the structure of the final compositions. Polyamide 6 may crystallize in three crystal forms: a stable phase α, a metastable phase β, and an unstable phase γ. Phase α is formed by arrangement of chains in regular conformations (all trans), while phase γ is a quasi-hexagonal structure form, in which the chains are helically twisted due to an irregular arrangement of intermolecular hydrogen bonds between amide groups. The meta-stable phase β is a rare intermediate phase from phase α to γ, or vice versa [17–19]. In Fig. 2 diffractograms of polyamide 6 and three PA6/OMMT composites are presented. In a 2θ angle range of 20–24°, one may observe reflections that come from the crystal phase of polyamide 6.

The most intense maximum around the angle 2θ = 21° stands for the created phase α100. The intensity of this reflection increases together with the addition of layered silicate to the matrix, which would suggest that the presence of a filler helps in creating a stable phase α. The conducted deconvolution of curves (Fig. 3) reveals the presence of other reflections. For polyamide 6 there is an overlap of five reflections, while the maximum angle 2θ at 13.6 and 22.0° occurs due to the presence of phases γ020 and γ001, accordingly. Reflection around the angle 2θ 23° indicates the presence of phase α002/202. The distribution of phases α and γ analysed

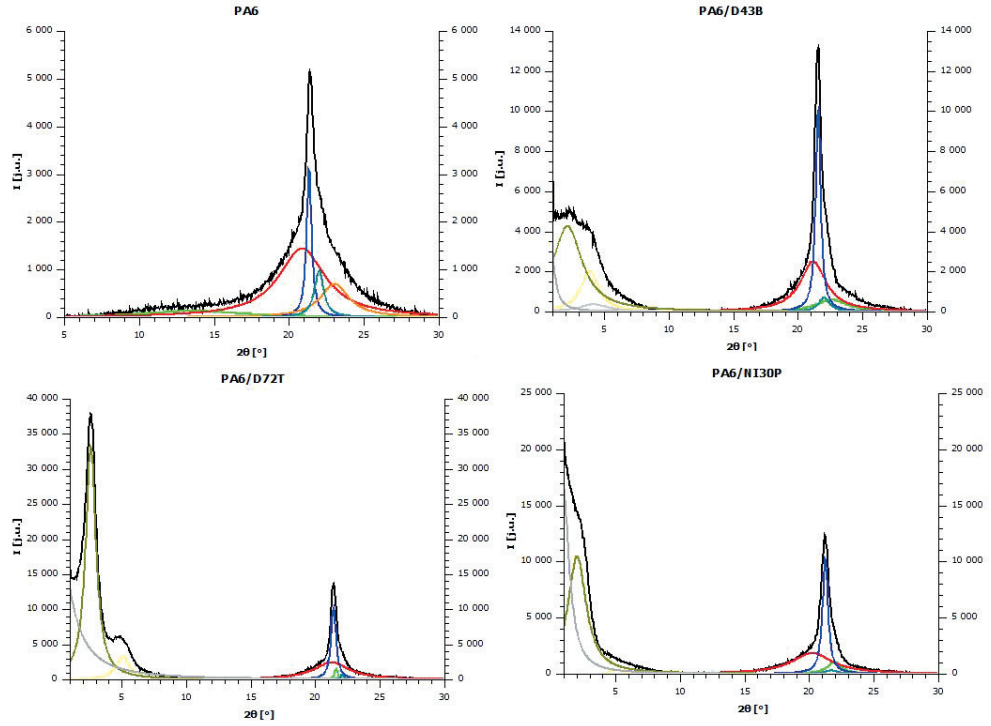

Fig. 3. PA6 and PA6/OMMT diffractograms with deconvolution results

Table 3. Crystallinity degree and interplanar distances determined for PA 6 and PA6/OMMT nanocomposites

Sample	Reflex No	2 Theta [°]	d [nm]	X_c [%]
PA6	1	13.6	0.65	39.8
	2	20.8	0.43	
	3	21.3	0.42	
	4	22.0	0.40	
	5	23.0	0.39	
PA6/D43B	1	0.7	12.86	53.7
	2	2.1	4.13	
	3	3.9	2.29	
	4	4.2	2.11	
	5	21.2	0.42	
	6	21.6	0.41	
	7	22.0	0.40	
	8	22.6	0.39	
PA6/D72T	1	2.6	3.38	40.8
	2	5.1	1.73	
	3	21.2	0.42	
	4	21.4	0.42	
	5	21.6	0.41	
	6	22.1	0.40	
PA6/NI30p	1	0.9	9.77	49.9
	2	2.0	4.37	
	3	5.1	1.74	
	4	20.2	0.44	
	5	21.2	0.42	
	6	21.7	0.41	
	7	21.9	0.41	

in this case is slightly different from that described in Ref. [18, 19]. In the quoted publications, the contribution of phase γ was more visible, while the addition of clay had a significant influence on the initiation of creating a phase that would be less thermodynamically stable. In Ref. [20] it has been suggested that the addition of layered silicate forces amide groups to be placed beyond the layer created by the chains. Thus, conformation changes of chains occur, which limits the creation of hydrogen bonds and the appearance of phase γ. In the diffractograms, elaborated as part of our research, the contribution of phase γ is minimal and visible only after performing the deconvolution. In the case of all of the compared material (regardless the clay used), the contribution of phase α was predominant, while the addition of layered silicates caused a decreased intensity of reflections originating from phase γ.

The interplanar distance of the organic clays was calculated as:

- For Dellite® 43B – reflection at 6.0° corresponds to interplanar distance of 1.47 nm;
- Dellite® 72T – reflection at 5.8° corresponds to interplanar distance of 1.52 nm;
- Nanomer® I30P - reflection at 8.9° corresponds to interplanar distance of 0.99 nm.

For PA6/OMMT systems (Dellite® 43B), the presence of a wide band of reflections at 0.7, 2.1, 3.9 and 4.2 of the 2θ angle suggests an efficient separation of montmorillonite layers in the range of 2.1–12.9 nm.

Implementation of Dellite® 43B and Nanomer® I30P organoclay helps in the creation of a polyamide nanocomposite with a large degree of separation of the clay layers, which suggests the presence of partial exfoliation of OMMT layers in the matrix. The presence of the preferred exfoliated structure results in an enhancement of physical and mechanical properties of a polymer nanocomposite [17–20].

The performed deconvolution of diffractograms has also enabled separation of signals from the amorphous and crystal phase of polyamide 6. Thus, according to the procedure described in Refs. [17–20], it was possible to calculate the crystallinity of polyamide 6 in the compositions analysed. In Table 3, the maximum reflections and their corresponding interplanar distances have been presented on the basis of the Bragg equation, as well as the crystallinity degree. The crystallinity degree of a pure matrix was 39.8%. The addition of 3% (m/m) of Dellite® 43B and Nanomer® I30P montmoryllonite has increased the degree of crystallinity by almost 10%.

3.3. Infrared spectroscopy (IR)

The IR spectra of polyamide composites (Fig. 4) reveal strong bands due to vibration of N-H and C=O bonds, which are characteristic of secondary amides:

- ν = 3330-3050 cm^{-1} band of N-H bonds vibrations,
- ν = 2950-2800 cm^{-1} band of C-H bonds vibrations,
- ν = 1680-1630 cm^{-1} band of C=O bonds vibrations,
- ν = 1560-1510 cm^{-1} band of N-H bond deformations,

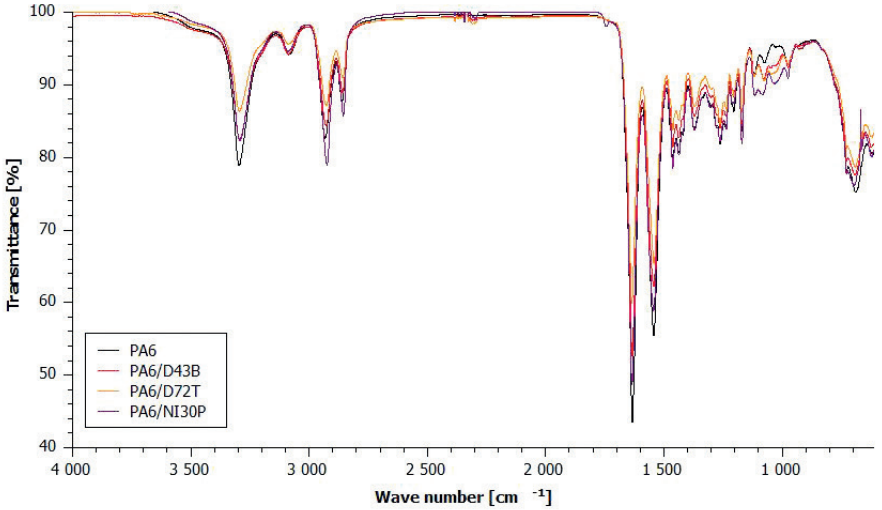

Fig. 4. IR spectra of PA6 – black curve; PA6/D43B – red curve; PA6/D72T – orange curve; PA6/NI30P – blue curve

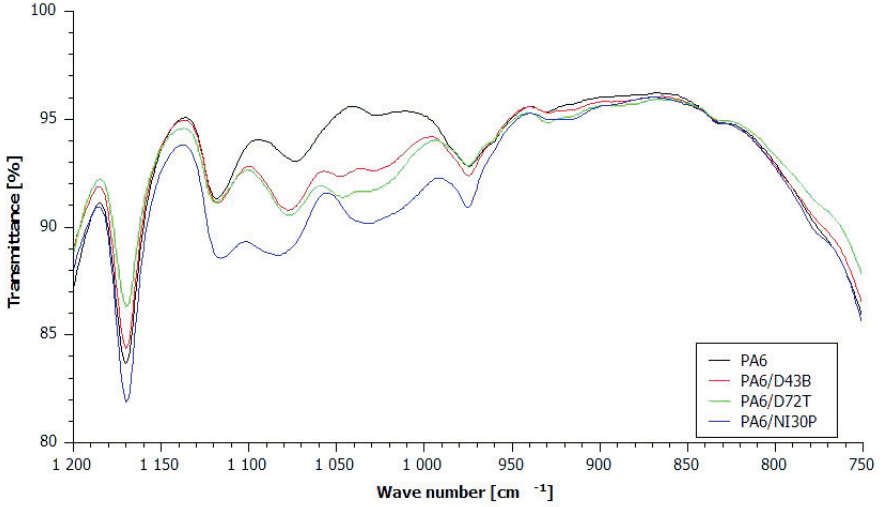

Fig. 5. IR spectra of PA6 – black curve; PA6/D43B – red curve; PA6/D72T – orange curve; PA6/NI30P – blue curve in the range of 1200-750 cm^{-1}

On the IR spectra of polyamide composites in the range of wave numbers of 1200-930 cm^{-1} (Fig. 4), there are bands related to vibrations of the CONH group in the plane that is applied for determination of the crystallinity degree of a polyamide. Fig. 5 shows the IR spectra in the range of wave numbers of 1200-750 cm^{-1} of polyamide 6 and PA6/OMMT nanocomposites. Bands at ν = 1029 and 928 cm^{-1} are connected with the contribution of the

crystal phase α and γ. The weak band at ν = 960 cm^{-1} is linked with the contribution of the crystal phase α. The band at ν = 975 cm^{-1} is connected with the contribution of crystal phase γ. The band at ν = 1120 cm^{-1}, as amorphous band, occurs in all of the composites analysed and may be used as a reference band during the determination of the crystallinity degree [21].

The following values of absorbancy were acquired in order to calculate the crystallinity degree:

- Aα - band of phase α and γ at ν = 929 cm^{-1}
- Aγ - band of phase α and γ at ν = 975 cm^{-1}

The crystallinity degree (X_c) was calculated from the following equation [21]:

$$Xc = 58.82 \cdot K + 32.06 \quad (1)$$

where: $K = A\alpha + 2/3 \cdot A\gamma$

Then, the contribution of phases α and γ has been calculated from the following equations [21]:

$$X\alpha = 10.76 \cdot \ln(A\alpha) + 57.37 \quad (2)$$

$$X\gamma = Xc - X\alpha \quad (3)$$

The acquired values for the total crystallinity degree and the crystallinity degree of phases α and γ for respective polyamide materials have been presented in Table 4.

The characteristic absorption bands from phase α are 1463 cm^{-1} (scissoring vibrations of CH_2 group), 1419 cm^{-1} (scissoring vibrations of CH_2 group), 1373 cm^{-1} (wagging vibrations from amide III and CH_2 group), 1204 cm^{-1} (twisting vibrations of CH_2 group), 959 cm^{-1} (deformation vibrations in plane CO-NH), 928 cm^{-1} (deformation vibrations in plane CO-NH). The characteristic absorption bands for phase γ have been noted at 1437 cm^{-1} (scissoring vibrations of CH_2 group), 1373 cm^{-1} (wagging vibrations of CH_2 group), 1237 cm^{-1} (twisting vibrations of CH_2 group), 975 cm^{-1} (deformation vibrations in plane CO-NH) and 725 cm^{-1} (vibrations from amide V group) [21].

3.4. Differential Scanning Calorimetry

For the DSC analysis PA6/OMMT composites with three types of nanofiller (Dellite 43B, Dellite 72T and Nanomer I30Pm) and a reference PA6 were applied. In Fig. 6 DSC the curves obtained at a heating rate of 20°/min and cooling rate of 5°/min are shown. The glass transition temperature, the temperatures for melting of crystal phases, changes of melting enthalpy, the specific heat, the temperature of crystallization and the crystallinity degree have been determined in accordance with the procedure described in [22, 23] and presented in Table 4.

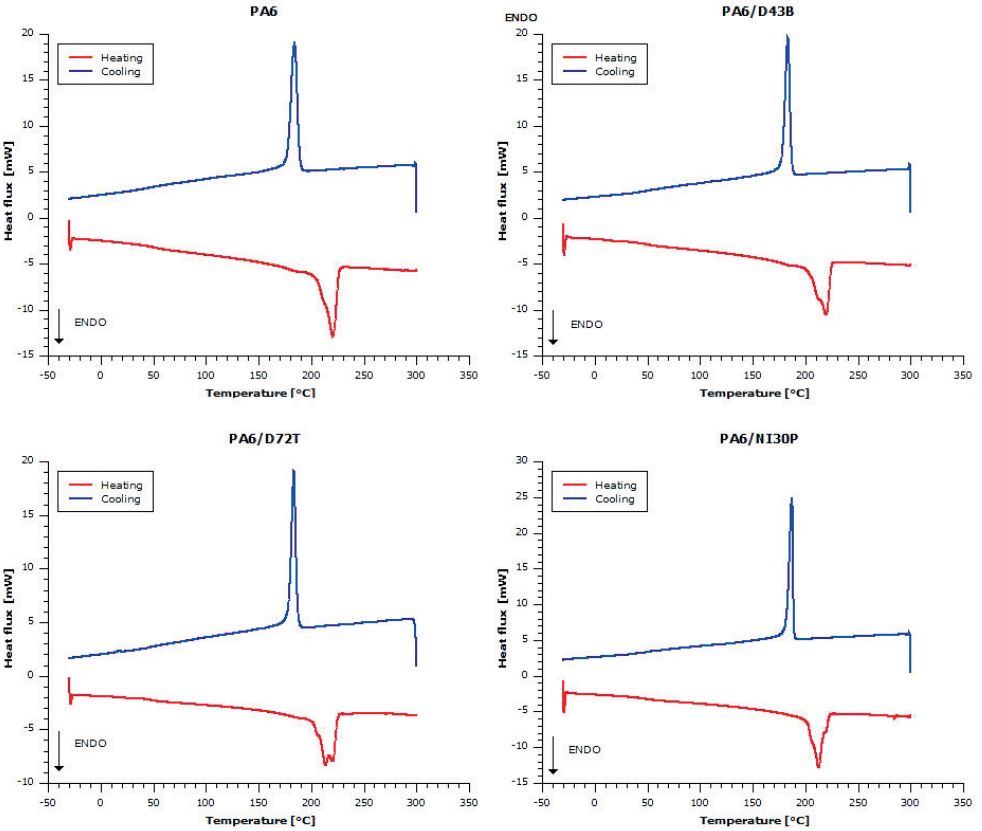

Fig. 6. DSC thermograms of polyamide 6 and PA6/OMMT composites

Table 4. Glass transition temperatures (Tg); melting temperature Tm; change of melting enthalpy ΔHm; change of specific heat ΔCp; crystallinity degree Xc and crystallization temperature Tc and change of crystallization enthalpy ΔHc for PA6 and PA6/OMMT composites

Sample	Tg [°C]	Tm [°C]	ΔH_m [J/g]	ΔCp [J/gK]	X_c [%]	T_c [°C]	ΔH_c [J/g]
PA6	49	220	80.38	0.260	33.49	184	69.92
PA6/D43B	49	220	72.26	0.224	31.04	184	65.14
PA6/72T	48	214	61.24	0.196	26.31	184	63.30
PA6/NI30P	48	214	67.46	0.244	28.98	187	63.47

On the basis of the DSC analyses conducted it can be found that the implementation of OMMT had almost no influence on the glass transition temperature (Tg) of the polyamide matrix, neither did it change the temperature at which the crystallization occurred at its maximum speed. Moreover, ΔCp and ΔHm decreased. These observations suggest that the

addition of aluminosilicate helps in the transition from the glass state into the elastic state, since significantly less heat is required for the system in order to achieve the transition point between those two states. The presence of 3% weight of organoclay resulted also in lowering the Xc value. Depending on the nanofiller used, various values of crystallinity degree have been noted. The rather slow cooling of samples, however, caused a small decrease of the contents of the crystal phase of the nanocomposite, despite its crystallization capacity. This may suggest that the formation of the amorphous phase of polyamide 6 depends on the type of organic modifier present in the composite system.

3.5. Mechanical properties (Flexural strength)

The maximum value of bending stress acquired from charts $\sigma = f(\varepsilon)$ (Fig. 7) for static bending resistance tests of polyamide 6 and two types of PA6/OMMT nanocomposites that were performed at temperatures of 0, 25 and 80°C have been described in Fig. 8 and Table 5.

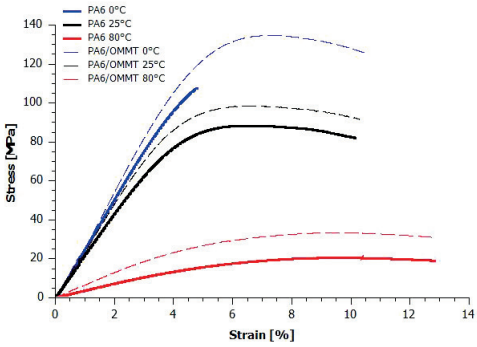

Fig. 7. Chart of dependencies in the deformation function for PA6, PA6/D43B and PA6/D72T performed at 0, 25 and 80°C

In the glass and brittle state at temperature of 0°C, due to a strong firmness, the bending stress increases rapidly along with the increase of deformation. The dependency described for polyamide 6 indicates a linear manner until the time of destruction. At a temperature of 0°C, the mobility of PA6 chain segments is rather minor and the applied bending strength causes the occurrence of small elastic stress. The organization of chains towards the stress is, in these conditions, more difficult and, after exceeding the critical point, there is a direct breaking of bonds in the macrochain. The addition of nanofiller causes not only an increase in its resistance against the strength applied, but is the factor which protects the structure against appearance of microfractures that would start the destruction process. While analysing the curve $\sigma = f(\varepsilon)$, it may be assumed that the material enforced with montmorillonite resembles a tendency to change its state from glass and brittle into a pseudo-elastic one. This may be caused by the fact that dispersed organoclay absorbs part of the bending strength applied on the surface of a particular sample and, due to this fact, the material shows a higher resistance to static bending. Together with the increase of the used strength, there is a certain maximum capacity of energy

that may be stored by the nanoparticles stored in the matrix. After this capacity is exceeded, the resistance becomes successively lower, together with an increase of deformation.

In the area of the glass state with forced flexibility at the temperature of 25°C, the dependency $\sigma = f(\varepsilon)$ also shows a linear character and, then, the curve is marked due to the occurrence of gaps and stress cracks in the micro-deformed area. Then, the effect of flow towards the cold is present and caused by the orientation processes of polymer chains. In the case of the tests for static bending resistance, the percentage of deformation is lower than in the case of static tensile resistance testing. Tests are ended after exceeding 7% deformation from the maximum point.

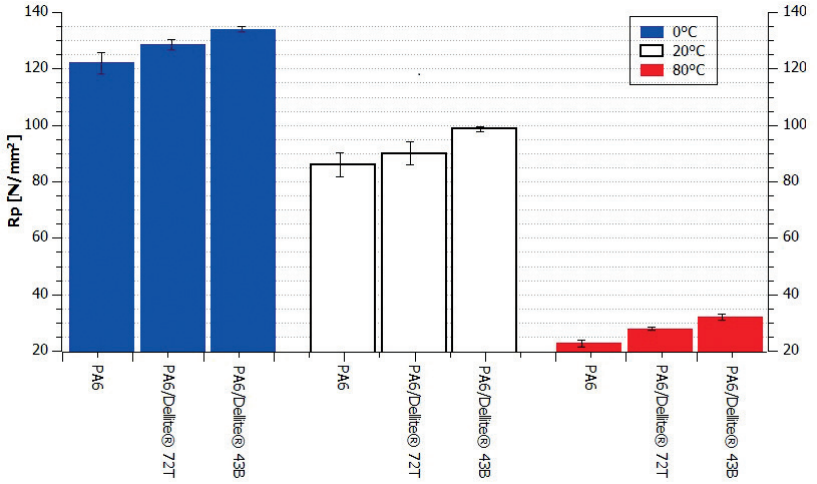

Fig. 8. Resistance against static bending (Rp) of PA6, PA6/D43B and PA6/D72T at various measuring temperatures

Table 5. Mechanical factors of PA6/MMT nanocomposites at various measuring temperatures: ε_f - bending modulus, σ_{fC} – flexural bending stress, ε_{fM} – elongation area at the bending strength, σ_{fB} – the bending stress at failure ε_{fB} – elongation area at the at failure

Sample	Temperature [°C]	ε_f [MPa]	σ_{fC} [MPa]	ε_{fM} [%]	σ_{fB} [MPa]	ε_{fB} [%]
PA6	0	2464	90.66	7.20	113.4	10.2
PA6/D43B		2832	101.18	6.98	124.6	10.0
PA6/D72T		2720	98.78	7.12	119.6	10.0
PA6	20	2022	69.76	7.08	80.0	10.4
PA6/D43B		2528	82.60	6.36	91.8	10.2
PA6/D72T		2304	75.68	6.68	83.8	10.4
PA6	80	384	13.74	10.14	21.1	13.0
PA6/D43B		682	21.78	9.10	29.8	12.4
PA6/D72T		558	18.12	9.56	25.9	13.0

When the temperature increases above the temperature of glass transition (test temperature equal 80°C), the polymer enters into a highly elastic range, becoming soft and flexible. In the range of small deformations, the stress-deformation curve is a linear process type, with a smaller module of E Young than in the state of forced elasticity in temperature of 25°C. The polymer becomes deformed when there is a fixed stress strength. Increase of temperature above Tg is advantageous for the mobility of segments of polymer chains and, different from the curve determined in ambient temperature, in a highly elastic area the stress increases monotonically, but non-linearly, along with the deformation. The elastic effects connected with entropic elasticity and the adhesive and elastic effects perform a predominant role.

3.6. Biotic degradation

Mechanical strength tests of composite materials, after their biotic degradation caused by biological factors – mainly enzymes produced by microbes, allows evaluation of the resistance of the material against biotic degradation. Tests have been conducted for 475 days in fertile soil of pH=6.8. Polyamide composites with layered silicate undergo a partial biological degradation that leads to worsening of mechanical properties. Results of the maximum stress of samples exposed to biotic degradation compared with the stress values of reference samples have been presented in Fig. 9 and Table 6.

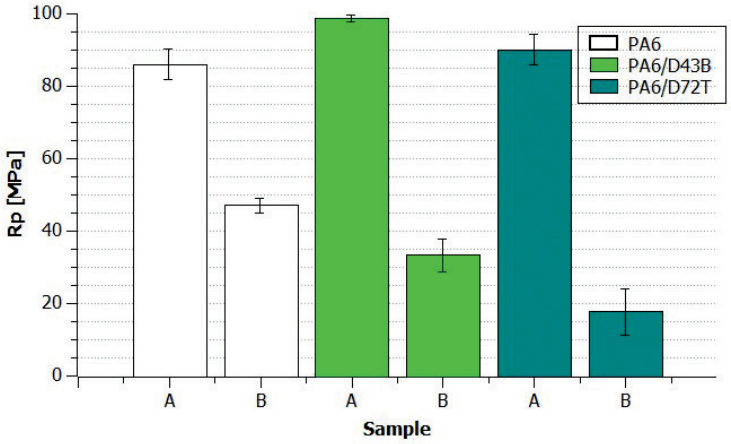

Fig. 9. Maximum stress (Rp) of reference samples (A) compared with the stress values of samples exposed to biotic degradation (B)

These results suggest that the maximum stress of PA6/OMMT composites after biotic degradation is significantly smaller than in the case of the reference material. It may be assumed that hydrolysis processes in the presence of organoclay play a key role. Adsorption and desorption processes in conditions of cyclic soaking and drying of the material are more intense than in the case of unmodified PA6. They lead to the creation of internal mechanical stress. Water helps microbes to develop and is advantageous for the enzyme reactions which

Table 6. Mechanical factors of PA6/MMT nanocomposites exposed to biotic degradation: ε_f – bending modulus, σ_{fC} – flexural bending stress, ε_{fM} – elongation area at the bending strength, σ_{fB} – the bending stress at failure, ε_{fB} – elongation area at the at failure

Sample	ε_f [MPa]	σ_{fC} [MPa]	ε_{fM} [%]	σ_{fB} [MPa]	ε_{fB} [%]
PA6	698	---	6.9	40	6.9
PA6/D43B	488	---	5.8	32	6.1
PA6/D72T	246	---	3.2	18	3.2

cause the microbiological degradation. Then, the influence of biological factors causes degradation of organic compounds into simple molecules in an enzymatic manner [24–28].

The variable results of static bending resistance may be caused by different chemical activity in which the components of the composite analysed serve as the feed for microbes or in which dissimilation processes occur, as a result of which the composite material is destroyed chemically by the substances produced and precipitated by microbes. Among the materials analysed, the sample with 3% content of clay organofilized with dimethyl benzyl ammonium salt had the highest Rp (flexural strength) value. The results clearly indicate that biological degradation of the polyamide sample was the smallest. The lowest resistance was noticed in the PA nanocomposite with montmorillonite organofilized with dimethyl ammonium salt with two long hydrocarbonic chains. The samples with organoclay were much more biologically active than the samples of pure polyamide 6. An increase in biological activity could be caused not only by the presence of a layered silicate, but also quaternary amphifilic salt and a small amount of chloride ions. Long exposure of nanocomposite samples in a strongly biological environment has created an opportunity for organoclay to react/interact with organic and non-organic compounds present in soil. Apart from strictly biological factors, such as the presence of microbes, synergistic factors co-responsible for lowering of mechanical properties of those materials one may include rapid cyclic temperature changes, absorptivity of water and other compounds in soil.

From technological point of view, knowledge about biotic degradation is important as it may limit further applications in e.g. the building industry and infrastructure sector. After 475 days the mechanical properties of PA6/MMT nanocomposites decreased to values similar to those presented in Ref. [29], where PA6/clay nanocomposites were flushed in deionized water. For future developments, polyamide 6/clay nanocomposites could be considered as useful tools for the design of environmental or medical markers, capable of detection of specific interactions with biological species.

4. Conclusions

The influence of the three types of organoclays modified with dimethyl-benzyl-hydrogenated tallow ammonium and dimethyl-di(hydrogenated tallow) ammonium salt on the physical properties of polyamide 6 nanocomposites was studied. X-ray diffraction results showed that in the presence of each type of nanofiller formation of a stable α phase of PA6 is

facilitated, whereby the amount of γ phase is minimal and visible only after deconvolution. For all the materials compared, the presence of α phase was dominant, and the addition of phyllosilicates caused a reduction in the intensity of reflections derived from γ phase. The incorporation of any of the fillers did not affect glass transition temperature. Regardless of the testing temperature, composites reinforced with dimethyl-benzyl-hydrogenated tallow ammonium-modified montmorillonite were characterized by the highest mechanical strength. This can be explained by the presence of the aromatic ring in the structure of the quaternary salt that affects the stiffness of the composite structure and resulting flexural strength.

During the biotic degradation as a result of absorption and desorption of water under cyclic soaking and drying of the material, swelling and contraction leads to the formation of internal mechanical stresses. Pristine polyamide was the most stable material against biological degradation and the PA composite with 3% content of clay organofilized with dimethyl benzyl ammonium salt had the highest Rp value; one can point to the role of the organomodifier when analysing this effect.

The research (work) was supported by the European Union through the European Social Fund within "Cracow University of Technology development programme – top quality teaching for prospective Polish engineers; University of the 21st century" project (contract no.UDA-POKL.04.01.01-00-029/10-00).

References

[1] Scala E.P., *A Brief History of Composites in the U.S.—The Dream and the Success,* Journal of the Minerals, Metals and Materials Society, 48(2), 1996, 49–48.

[2] Pavlidou S., Papaspyrides C.D., *A review on* polymer-*layered silicate nanocomposites*, Progress in Polymer Science, 33, 2008, 1119–1198.

[3] Ray S.S., Okamoto M., *Polymer/layered silicate nanocomposites: a review from preparation to processing*, Progress in Polymer Science, 28, 2003, 1539–1641.

[4] Leszczyńska A., Njuguna J., Pielichowski K., Banerjee J.R., *Polymer/ montmorillonite nanocomposites with improved thermal properties Part II*, Thermochimica Acta, 454, 2007, 1-22.

[5] Leszczyńska A., Njuguna J., Pielichowski K., Banerjee J.R., *Polymer/ montmorillonite nanocomposites with improved thermal properties Part I,* Thermochimica Acta, 453, 2007, 75.

[6] Leszczyńska A., Pielichowski K., *Application of thermal analysis methods for characterization of polymer/montmorillonite nanocomposites,* Journal of Thermal Analysis and Calorimetry, 93(3), 2008, 677–687.

[7] Pielichowski K., Leszczyńska A., *Polyoxymethylene-based nanocomposites with montmorylonite: oan introductory study,* Polimery, 2, 2006, 60–66.

[8] Vaccari A., *Clays and catalysis: a promising future,* Applied Clay Science, 14, 1999, 161–244.

[9] Kim N.H., Malhotra S.V., Xanthos M., *Modification of cationic nanoclays with ionic liquids*, Microporous Mesoporous Materials, 96, 2006, 29.

[10] Morfis S., Philippoulos C., Papayannakos N., *Application of Al-pillared clay minerals as catalytic carriers for the reaction of NO with CO*, Applied Clay Science, 13, 1998, 203.
[11] Christidis G.E., Scott P.W., Dunham A.C., *Acid activation and bleaching capacity of bentonites from the islands of Milos and Chios, Aegean, Greece*, Applied Clay Science, 12, 1997, 329.
[12] Duleba B., Spišák E., Greškovič F., *Optimization of injection molding process by DOE*, Procedia Engineering, 96, 2014, 75–80.
[13] Wu S., Jiang D., Ouyang X., Wu F., Shen J., *The structure and properties of PA6/MMT nanocomposites prepared by melt compounding*, Polymer Engineering & Science, 44, 2004, 2070–2074.
[14] Kherrou D.E., Belbachir M., Lamouri S., Bouhadjar L., Chikh K., *Synthesis of Polyamide-6/Montmorillonite Nanocomposites by Direct In-situ Polymerization Catalysed by Exchanged Clay*, Oriental Journal of Chemistry, 29(4), 2013, 1429–1436.
[15] Stoeffler K., Utracki L.A., Simard Y., Labonte S., *Polyamide 12 (PA12)/clay nanocomposites fabricated by conventional extrusion and water-assisted extrusion processes*, Journal of Applied Polymer science, 130(3), 2013, 1959–1974.
[16] Dintcheva Z.T., Filippone G., Arrigo R., La Mantia F.P., *Low-Density Polyethylene/Polyamide/Clay Blend Nanocomposites: Effect of Morphology of Clay on Their Photooxidation Resistance*, Journal of Nanomaterials, vol. 2017, Article ID 3549475, 2017, 9, doi:10.1155/2017/3549475.
[17] Rotter G., Ishida H., *FTIR separation of nylon-6 chain conformations: Clarification of the mesomorphous and γ-crystalline phases*, Journal of Polymer Science Part B, 30, 1992, 489.
[18] Goderis B.,Klein P.G., Hill S.P., Koning C.E., *A comparative DSC, X-Ray and NMR study on the crystallinity of isomeric aliphatic polyamides*, Progress in Colloid and Polymer Science, 130, 2005, 40–50.
[19] Liu T.X., Liu Z.H., Ma K.X., Shen K.Y., He C.B., *Morphology, thermal and mechanical behavior of polyamide 6/layered-silicate nanocomposites*, Composites Science and Technology 63, 2003, 331–337.
[20] Lincoln D.M., Vaia R.A., Wang Z.G., Hsiao B.S., *Secondary structure and elevated temperature crystallite morphology of nylon-6/layered silicate nanocomposites*, Polymer, 42, 2001, 1621.
[21] Hanna A.A., *Thermal and dielectric properties of nylon 6*, Thermochimica Acta, 76, 1984, 97–103.
[22] Wu Q., Liu X., Berglund L.A., *FT-IR spectroscopic study of hydrogen bonding in PA6/clay nanocomposites*, Polymer 43(8), 2002, 2445–2449.
[23] Katoh Y., Okamoto M., *Crystallization controlled by layered silicates in nylon 6–clay nanocomposite*, Polymer, 50, 2009, 4718–4720.
[24] Kaczmarek H., Bajer K., *Metody badania biodegradacji materiałów polimerowych*, Polimery, 51(10), 2006, 13–18.
[25] Foltynowicz Z., Jakubiak P., *Poli(kwas mlekowy) – biodegradowalny polimer otrzymywany z surowców roślinnych*, Polimery, 47, 2002, 11–12.

[26] Pielichowski K., Majka T.M., Leszczyńska A., Giacomelli M., *Optimization and Scaling up of the Fabrication Process of Polymer Nanocomposites*: *Polyamide 6/Montmorillonite Case Study*; Springer-Verlag Berlin Heidelberg, in. Niuguna J. (Ed) Structural Nanocomposites, 2013, 75–103.
[27] Majka T.M., Bartyzel O., Raftopoulos K.N., Pagacz J., Leszczyńska A., Pielichowski K., *Recycling of polypropylene/montmorillonite nanocomposites by pyrolysis*, Journal of Analytical and Applied Pyrolysis, 119, 2016, 1–7.
[28] Majka T.M., Leszczyńska A., Kandola B.K., Pornwannachai W., Pielichowski K., *Modification of organo-montmorillonite with disodium H-phosphonate to develop flame retarded polyamide 6 nanocomposites,* Applied Clay Science, 139, 2017, 28–39.
[29] Majka T.M., Pielichowski K., Leszczyńska A., *Wpływ chłonności płynów eksploatacyjnych stosowanych w motoryzacji przez kompozyty PA-6/MMT na ich właściwości mechaniczne*, Czasopismo Techniczne, 9-M/2012, 147–154.